Biomedical Spectroscopy and Imaging 3 (2014) 293–300
DOI 10.3233/BSI-140085
IOS Press

Imaging of nonlinear microscopy of burned skin treated by ultra-high intensity laser pulses

Moises Oliveira dos Santos [a,b], Carolina Benetti [b], Vitor Bianchin Pelegati [c], Carlos Lenz Cesar [c], Wagner de Rossi [b], Ricardo Elgul Samad [b], Nilson Dias Vieira, Jr. [b], Telma Maria Tenório Zorn [d] and Denise Maria Zezell [b,*]

[a] *Escola Superior de Tecnologia, State University of Amazonas, Manaus, Brazil*
[b] *Centre for Lasers and Applications, Nuclear and Energy Research Institute, São Paulo, Brazil*
[c] *Instituto de Física "Gleb Wataghin", State University of Campinas, Campinas, Brazil*
[d] *São Paulo University, São Paulo, Brazil*

Abstract.
BACKGROUND: The techniques of second harmonic generation (SHG) and two-photon excitation of fluorescence microscopy (TPEFM) have shown as powerful tools to investigate collagen and extracellular matrix components.
OBJECTIVE: The aim of this study is evaluate the feasibility of using femtosecond lasers of high intensity as an auxiliary treatment of burn patients using an *in vivo* model, monitoring and characterizing the healing process by histology and SHG + TPEFM.
METHODS: Samples from three dorsum areas of Wistar rats anaesthetized were burned by water vapour exposure and treated by debridement and laser ablation at the third day post burned. To differentiating the healing process, skin fresh biopsies at four different days of study were evaluated by histology, TPEFM and SHG.
RESULTS: Changes in the skin caused by vapour exposure were observed by histological images and characterized by TPEFM + SHG images. The healing process of burned skin was observed by regeneration of its morphology comparing histological images. The integrity of collagen and components of extracellular matrix are evidence of a normal skin detected by TPEFM + SHG.
CONCLUSIONS: The methods used to characterize the tissue are useful to validate the femtosecond lasers ablation treatment of burned skin.

Keywords: Burned skin, ultra-high intensity laser pulses, nonlinear microscopy

1. Introduction

Burns destroy the barrier function of skin. In 2012 in the United States, 450,000 people received medical treatment, per year, 3,400 peoples die from burns and fire [1]. The burns are classified into causal categories, injury zones and depth [3]. The reduction of mortality is related to several factors: effectiveness of early protection of the burned area; reducing the metabolic effort of the patient and infection control [2]. The current therapy includes evaluation, treatment and rehabilitation. Once the wound was evaluated, depth determined, cleaned and debrided, treatment begins [20].

*Corresponding author: Denise Maria Zezell, Centre for Lasers and Applications, Nuclear and Energy Research Institute, Av. Prof. Lineu Prestes, 2242 – Cidade Universitária, São Paulo, Brazil. Tel.: +55 11 3133 9370; E-mail: zezell@usp.br.

A precise method to controlled remove tissue is by using ultrashort pulse lasers [6,14]. This ablation occurs when the beam intensity is above the threshold for tissue ablation causing a breaking of electronic bonds in the sample [7,18]. To characterize the degraded collagen after burn and to monitor the wound healing process after treatment with femtosecond laser, the study uses the methods of histology and nonlinear microscopy (SHG and TPEFM).

The histology is considered the gold standard in study of morphological of tissues and define the burn depth. The SHG technique allow to imaging of organization collagen and monitoring changes associated to injuries [17]. The TPEFM technique allow detect extracellular matrix components of skin which can emit fluorescence when excited [10].

The aim of the study is to evaluate the feasibility of using femtosecond lasers of high intensity as an adjunct in the treatment of burn patients using an *in vivo* model, monitoring and characterizing the healing process by histology and SHG + TPEFM.

2. Material and methods

2.1. Outline of study

The study for femtosecond laser validation for use in burns was developed according to experimental design: (i) the animals were anaesthetized and shaved; (ii) three regions were burned and one animal per group was chosen to control (normal skin); (iii) after three days (delimitation of the injury) one lesion was laser ablated, and other debrided, another not been treated, (iv) in the third, fifth, seventh and fourteenth day (study group) after treatment the animals were sacrificed and samples taken for analysis (histology, TPEFM and SHG).

2.2. Animal model

The Animal Research Ethical Committee approved the procedures used in this project. Wistar rats, males, adults, weighing of 200–250 g were housed and fed properly in individual cages under controlled temperature and light regime of 12 h/12 h during study. Before the burn procedures the rats were anaesthetized intramuscularly with ketamine (0.32 ml/kg) and xylazine (0.2 ml/kg) combination, shaved and region was washed. Three burn wounds were created with 8 mm diameter by exposure for 20 s to a vapor source prepared with a rubber tube attached to the outlet of steam.

2.3. Laser ablation

In this study the laser system used was a Ti:Sapphire main oscillator (Mira-Seed, Coherent) that generate ultrashort pulses which were amplified by a Ti:Sapphire CPA (chirped pulse amplification). The skin ablation threshold was defined in a pilot study as 2.21 J/cm^2 [16]. The energy per pulse used for ablation were 10 μJ, with pulses overlapping of 25%, sample displacement speed of 540 mm/min, and pulse repetition rate of 2 kHz. The laser beam was focused by a lens with 25.4 mm of diameter and a focal length of 50.0 mm. The samples were positioned and moved with a linear translation stage with 10^{-6} m resolution. For each sample the laser pulses energy was measured with a power meter (OPHIR PE50-SH-V2).

2.4. Histology

The entire wound and healthy part of the skin adjacent to edge of it was excised from the animal at the designated time point and half of the tissue was fixed in Methacarn solution (methanol and Carnoy solution), and maintained for a maximum of 3 h, according to protocol, after receiving the processing laboratory routine. The histological sections were performed transversally, stained with hematoxylin-eosin and examined under light microscope (Leica DMLP, Germany).

2.5. Nonlinear microscopy

The samples were obtained as described in Section 2.2. The samples were cryo-preserved and cut perpendicularly to the epidermis, using Cryomicrotome, comprising a cross section of epidermis and dermis layers with 20 μm of thickness mounted on slides and covered with cover slip for image acquisition. The images were obtained by the techniques of autofluorescence and second harmonic generation lacked markers of exogenous cells.

The sections mounted on slides were examined at the National Institute of Science and Technology Photonics Applied to Cell Biology (INFABIC), State University of Campinas, using confocal LSM 780-NLO – Zeiss Axio Observer Z.1 microscope (Carl Zeiss AG, Germany), using the lens with 40× and 10× magnification. Images were collected using a laser NLO – Mai Tai with a wavelength centered at approximately 950 nm for excitation and emission bandpass filters 520 nm to 560 nm for autofluorescence reflected and transmitted a low pass filter of 485 nm for detection of SHG reflected and transmitted with pinhole set to 1 airy unit in each channel image format 1024×1024 and 1× optical zoom. Z-stacks were acquired with an interval of 6.30 μs. The INFABIC is co-funded by the Research Foundation of the State of São Paulo – FAPESP (process: 08/57906-3) and National Council for Scientific and Technological Development – CNPq (process: 573913/2008-0).

2.6. Data analysis

The SHG images were analyzed by the function of Fast Fourier Transform – FFT, ImageJ 1.45s software (National Institutes of Health, USA) to calculate the collagen orientation index (COI) which is defined as [21]:

$$\mathrm{COI} = 1 - \frac{W}{H}, \tag{1}$$

where W and H represent the width and height of the ellipse or circle in the power plots of SHG images (Fig. 1). The COI ranging from 0 to 1. For collagen fibers with a parallel orientation, the index approaches to 1. In the collagen fibers that are randomly oriented, the orientation index tends to zero.

Once calculated the rates of collagen orientation, we calculated the arithmetic mean of each sample (burned, debrided and laser ablated) to identify the similarities and differences between the groups (Table 1).

2.7. Statistical analysis

Statistical analysis were performed using the GraphPad Prism 5. The groups went through the normal test method Kolgomorov–Smirnov. To analyze the results were used the ANOVA test and post-test Tukey for comparison between groups.

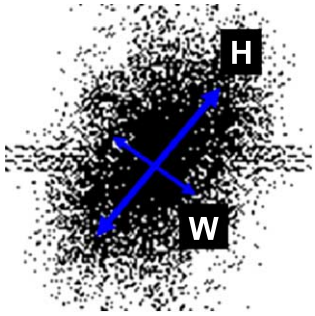

Fig. 1. Estimation of the collagen orientation by the ratio of width (W) by the length (H) of Fourier transform applied to the region of interest of the image (ROI). (Colors are visible in the online version of the article; http://dx.doi.org/10.3233/BSI-140085.)

Table 1
Collagen orientation index mean of each sample at days of monitoring

	Day 3	Day 5	Day 7	Day 14
Burned	0.369 ± 0.021	0.350 ± 0.053	0.518 ± 0.022	0.474 ± 0.024
Ablated	0.389 ± 0.002	0.328 ± 0.089	0.493 ± 0.038	0.393 ± 0.035
Debrided	0.410 ± 0.025	0.326 ± 0.066	0.442 ± 0.038	0.458 ± 0.037

3. Results and discussion

3.1. Histological analysis

The structure of skin is composed by three layers and derivative structures [5,9,13]. It has several functions and the most important is to form a physical barrier to the environment [3]. The summarize of histological images of normal skin and the changes in skin after burn and burn + treatments can seen in Fig. 2.

The image of normal skin shows a fairly consistent structure. A significantly epidermis, dermis, sebaceous glands, hair follicles and capillary vessels can be observed. After production of burn injury, a monitoring of the healing process by histological image of cross-section of the skin was performed and reported in Fig. 1. Significant changes are observed in the skin layers.

When compare an image of normal skin with a burned skin, a continuity solution in keratinized stratified epithelium on third day and an initial regeneration on the fifth day can be observed. During monitoring, a considerable amount of hair follicles with degraded shaft in cross section scattered throughout the dermis. In the end of monitoring, the epithelium presents with continuity solution reduced more distinction between the collagen fibers, fibroblasts more elongated nucleus denoting the quiescent state of the cell. The same results observed for the burned skin, was observed for debrided and laser ablated skin. In all images, the presence of fat cells near the epithelium migrating from hypodermis was observed. Studies in obese mice showed increased adipose tissue infiltration of macrophages and pro-inflammatory cytokines highlighting the inflammatory condition in the region, human studies have also reported similar results for the recruitment of macrophages by adipocytes [4,8,11].

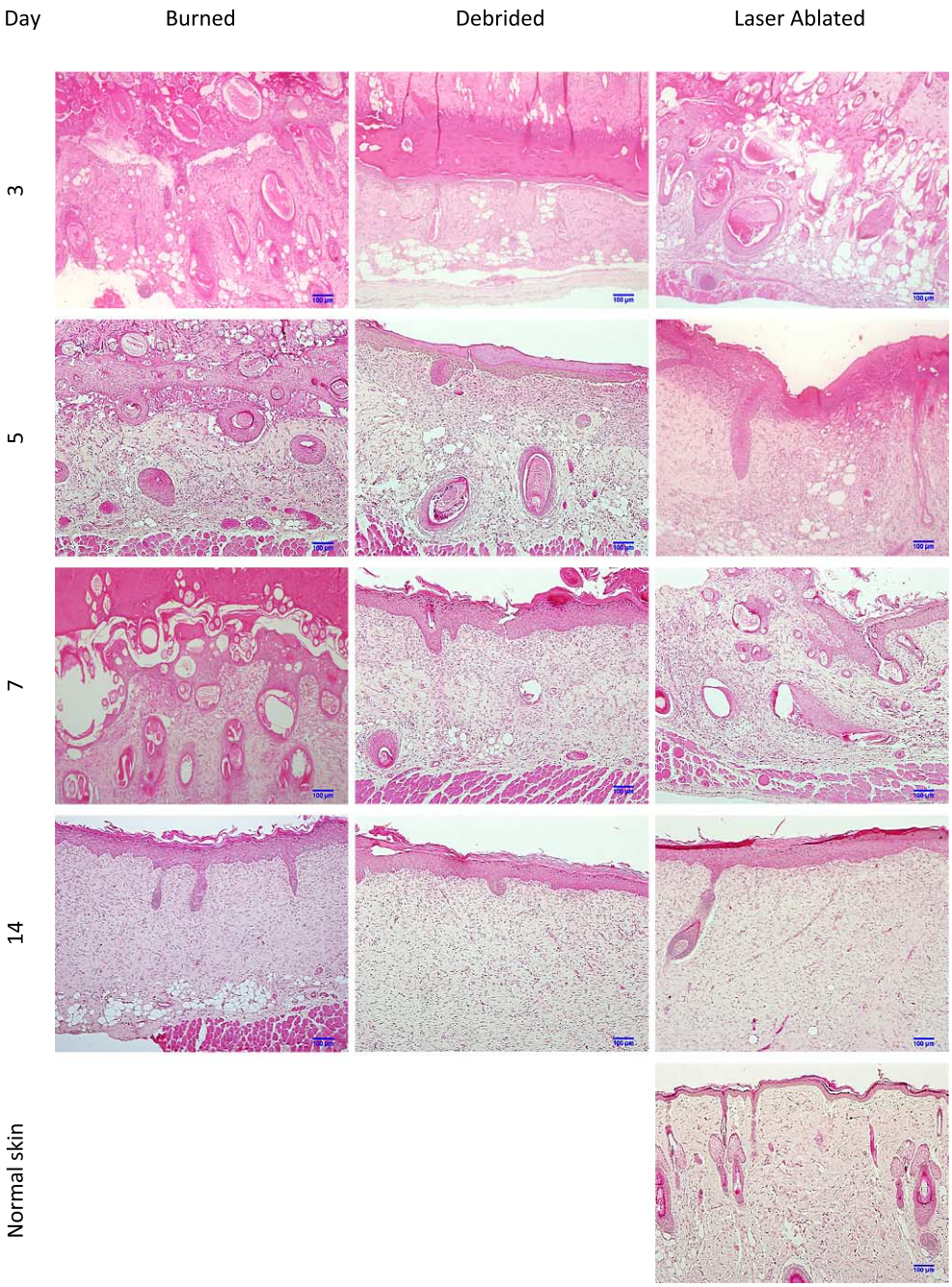

Fig. 2. Histological sections with a thickness of 5.0 μm, paraffin embedded and stained with hematoxylin-eosin. The lines shown the day of monitoring the healing process; column represent the conditions of skin: burned, debrided and laser ablated. In the last line is shown the normal skin of Wistar rats. 10× magnification. (Colors are visible in the online version of the article; http://dx.doi.org/10.3233/BSI-140085.)

3.2. Nonlinear microscopy analysis

In this section, we present the results obtained from SHG/TPEFM. In Fig. 3 representative SHG/TPEFM images of normal and injured skin can be observed. When comparing different images of SHG, we can observe a reduction of amount and distribution of collagen (red areas) in images. These results indicate a collagen degradation due to increase of temperature in burned site [7,14,18]. Over the monitoring days, red areas in SHG images increase appreciably. Analysis of images show a representative amount using COI [19,21]. The results demonstrated that collagen undergo an increase in the orientation over time and phases of wound healing. The comparison test among groups show no statistical difference at day 14.

A visual inspection of overlapping SHG and TPEFM images seems that amount of extracellular matrix components at the beginning of the monitoring rise over time, showing a tendency to return to normal skin [12,15,22].

4. Conclusion

Nonlinear microscopy images allowed an understanding of the physiological and morphological states of the tissue. Analyzing the images throughout the follow-up period of the healing process, we observed that the collagen that was degraded by increased temperature, was regenerated over time, as indicated by the amount of collagen in the images. The autofluorescence observed by TPEFM allowed to evaluate the morphological tissue regeneration, and establish hypotheses based on the emission band collected by the microscope, on which chromophores contribute to the fluorescence. In all samples, there was emitted fluorescence due to keratin, elastin and glycoproteins present in the dermis. Only on the seventh day of COI, it was not possible to observe the differences among treatments. After 14 days, for both treatments, collagen fibers have not yet reached the same organization of fiber in healthy skin. Histologically, the skin regeneration will not be different using scalpel debridement or laser ablation. After 14 days, for both treatments, collagen fibers have not yet reached the same organization of fiber in healthy skin. This could be explained because the maturation and remodeling of the scar begins during the fibroblastic phase and is characterized by reorganization of previously synthesized collagen and it continues for many (6–12) months post injury, gradually resulting in a mature scar [3]. Debridement is not a well-controlled method of tissue removal, while the volume and depth of tissue removal is predicted using femtosecond laser, allowing several scans, with no mechanical contact, virtually not depending on medical doctor skills and without infection risk.

The study provided support for the feasibility of using femtosecond lasers of high intensity as an adjunct in the treatment of burn patients by an *in vivo* model.

Acknowledgements

The authors would like to thank the funding agencies for financial aid for research: FAPESP/CEPID (05/51689-2); Instituto Nacional de Fotônica/CNPq (573.916/2008-0); CNPq (312397/2013-5); FAPEAM – Programa RH-POSGRAD.

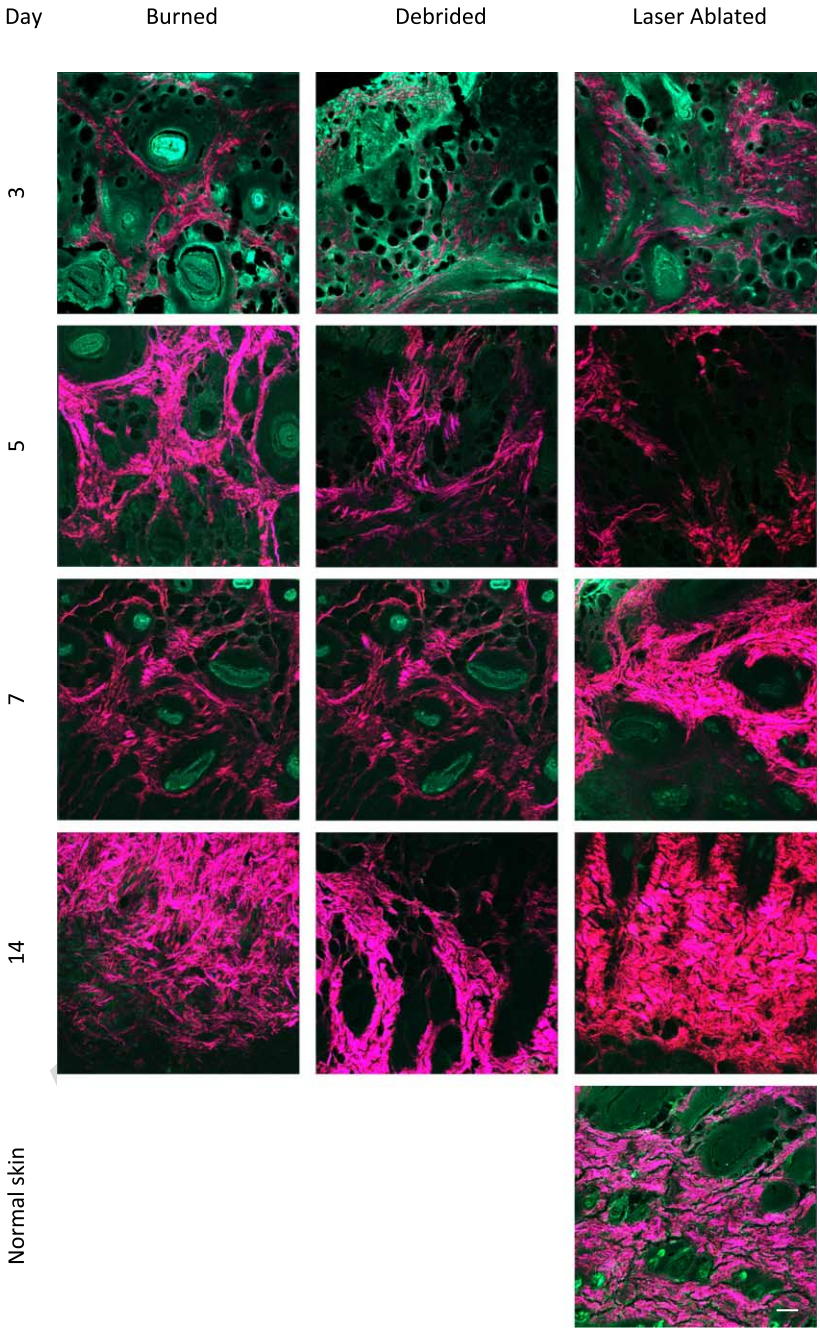

Fig. 3. Representative overlapping SHG/TPEFM images of perpendicular section of dermis with thickness of 20 μm. SHG signal are shown in red and TPEFM are shown in green. The lines shown the day of monitoring the healing process; column represent the conditions of skin: burned, debrided and laser ablated. In the last line is shown the normal skin of Wistar rats. Scale bar = 100 μm. 40× magnification. (The colors are visible in the online version of the article; http://dx.doi.org/10.3233/BSI-140085.)

References

[1] American Burn Association, Burn incidence and treatment in the United States: 2012, Fact sheet, available at: http://ameriburn.org.
[2] B.S. Atiyeh, S.W. Gunn and S.N. Hayek, State of the art in burn treatment, *World Journal of Surgery* **29** (2005), 131–148.
[3] F. Brunicardi, D. Andersen, T. Billiar, R. Pollock et al., *Schwartz's Principles of Surgery*, 9 edn, McGraw-Hill Professional, New York, 2009, Chapter 7.
[4] R. Cancello, C. Henegar, N. Viguerie et al., Reduction of macrophage infiltration and chemoattractant gene expression changes in white adipose tissue of morbidly obese subjects after surgery-induced weight loss, *Diabetes* **54** (2005), 2277–2286.
[5] D.E. Elder, B. Johnson, R. Elenitsas et al., *Lever's Histopathology of the Skin*, Lippincott Williams & Wilkins, 2008.
[6] D. Evison, R.F.R. Brown and P. Rice, The treatment of sulphur mustard burns with laser debridement, *Journal of Plastic, Reconstructive and Aesthetic Surgery* **V.59** (2006), p1087–p1096.
[7] K.S. Frederickson, E.W. White, R.G. Wheeland and D.R. Slaughter, Precise ablation of skin with reduced collateral damage using the femtosecond-pulsed terawatt Titanium:Sapphire laser, *Archives of Dermatology* **129** (1993), 989–993.
[8] D.T. Furuya, A.C. Poletto, R.R. Favaro, J.O. Martins, T.M. Zorn and U.F. Machado, Anti-inflammatory effect of atorvastatin ameliorates insulin resistance in monosodium glutamate-treated obese mice, *Metabolism* **59**(3) (2010), 395–399.
[9] L.P. Gartner and J.L. Hiatt, *Color Atlas and Text of Histology*, Lippincott Williams & Wilkins, 2003.
[10] S.W. Hell, Nonlinear optical microscopy, *Bioimaging* **4** (1996), 121–123.
[11] G.S. Hotamisligil, P. Arner, J.F. Caro, R.L. Atkinson and B.M. Spiegelman, Increased adipose tissue expression of tumor necrosis factor-alpha in human obesity and insulin resistance, *Journal of Clinical Investigation* **95**(5) (1995), 2409–2415.
[12] K.E. Kadler, D.F. Holmes, J.A. Trotter and J.A. Chapman, Collagen fibril formation, *Biochemical Journal* **316** (1996), 1–11.
[13] A.L. Kierszenbaum, *Histology and Cell Biology*, Elsevier, 2008.
[14] M.H. Niemz, *Laser–Tissue Interactions: Fundamentals and Applications*, Springer, 2007.
[15] R. Pankov and K.M. Yamada, Fibronectin at a glance, *Journal of Cell Science* **115** (2002), 3861–3863.
[16] M.O. Santos, A.Z. Freitas, R.E. Samad, D. Lacerda, T.M.T. Zorn, D.M. Zezell and N.D. Vieira, Third-degree burn treatment with ultrashort pulse laser debridement, *Lasers in Surgery and Medicine* **42**(22), (2010), 13–14.
[17] P.T.C. So, C.Y. Dong et al., Two photon excitation fluorescence microscopy, *Annual Review of Biomedical Engineering* **02** (2000), 399–429.
[18] B.C. Stuart, M.D. Feit, S. Herman, A.M. Rubenchik, B.W. Shore and M.D. Perry, Optical ablation by high-power short-pulse lasers, *Journal of Optical Society of America B* **13**(2) (1996), 459–468.
[19] P.P. van Zuijlen, J.J. Ruurda, H.A. van Veen, J. van Marle, A.J. van Trier, F. Groenevelt, R.W. Kreis and E. Middelkoop, Collagen morphology in human skin and scar tissue: no adaptations in response to mechanical loading at joints, *Burns* **29** (2003), 423–431.
[20] T.H. Wang, H. Ma, F.L. Yeh, J.T. Lin and B.H. Shen, The use of "composite dressing" for covering split-thickness skin graft donor sites, *Burns* **36**(2) (2010), 252–255.
[21] S. Wu, H. Li, H. Yang et al., Quantitative analysis on collagen morphology in aging skin based on multiphoton microscopy, *Journal of Biomedical Optics* **16**(4) (2011).
[22] X. Zhu, S. Zhuo, L. Zheng, K. Lu, X. Jiang et al., Quantified characterization of human cutaneous normal scar using multiphoton microscopy, *Journal of Biophotonics* **3**(1,2) (2010), 108–116.